Deuterium NMR Study of Molecular Dynamics and Phase Transition in Acetonitrile Crystal

You Suzuki, Masato Sato, Kazuyoshi Takanohashi, Tomonori Ida, and Motohiro Mizuno*

Department of Chemistry, Graduate School of Natural Science and Technology, Kanazawa University, Kanazawa, Ishikawa 920-1192, Japan

Received: July 22, 2008; Revised Manuscript Received: October 23, 2008

The molecular dynamics and local structure in the α and β phases of CD_3CN were studied by ^2H NMR spectroscopy. From the ^2H NMR spin−lattice relaxation time (T_1), the activation energies of the rotation of the CD_3 group about the C_3 axis in both phases were found to be 6.2 and 11 kJ mol^{-1}, respectively. These activation energy values suggest that the packing between CD_3CN molecules in the α phase is weaker than that in the β phase. The slow structural change of the crystal due to the α−β phase transition was investigated using the ^2H NMR spectra and T_1. A jump of CH_3CN between two neighboring sites in the hydrogen-bond network accompanying the molecular reorientation was observed by the ^2H NMR 2D exchange spectra and the stimulated-echo method in the α phase. Vacancy diffusion occurred in the one-dimensional hydrogen-bond network in the α phase.

1. Introduction

Acetonitrile, CH_3CN, is well-known as an important organic solvent. The melting point of CH_3CN is 227 K. In the solid state, CH_3CN exists in two forms, α and β, with a phase transition point at 216.9 K.[1] The structures of both phases have been analyzed by X-ray and neutron diffraction methods.[2−4] The structure of the CH_3CN crystal in the β phase is orthorhombic, space group $Cmc2_1$, and that in the α phase is monoclinic, space group $P2_1/c$. The CH_3CN molecules are stacked along a [010] axis and are packed in layers parallel to (100) in the β phase. The molecules are parallel in the same layer and are packed head-to-tail. The α−β phase transition accompanies a 90° rotation of alternate molecules in layers. The difference in the local structures of the α and the β phases have been studied using ^{14}N nuclear quadrupole resonance (NQR) spectroscopy.[5,6] The α−β phase transition of CH_3CN has been investigated by measurements of its heat capacity.[1] The α−β phase transition of CH_3CN takes place at a broad temperature range. The coexistence of the α and β phases around the α−β phase transition point has been reported.[1] The thermodynamic properties of the α−β phase transition are very complex because of the effects of premelting and a slow approach to equilibrium. Consequently, although several analyses of the α−β phase transition and the structures of each phase have been performed, the molecular dynamics in each phase and detailed properties of the α−β phase transition have not been investigated.

Solid-state ^2H NMR spectroscopy is effective for the study of molecular dynamics and the orientations of molecules.[7−30] Molecular motions in the range of 10^3-10^6 s^{-1} can be studied from the line shape analysis of the broadline ^2H NMR spectrum.[7−19] Information on molecular motions on a time scale of $<10^3$ s^{-1} can be obtained from 2D exchange ^2H NMR spectra and the stimulated-echo method.[7,19−30] Slow dynamics such as the vacancy diffusion in crystalline benzene have also been investigated by these methods.[25] Molecular motions on a time scale of $>10^7$ s^{-1} can be studied from the spin−lattice relaxation time (T_1).[8,9,16,19]

In the present work, we report an investigation of the local structure and molecular dynamics in the α and β phases using solid-state ^2H NMR spectroscopy. ^2H NMR T_1 exposes the variations in molecular packing and the fast molecular dynamics due to the α−β phase transition. In the α phase, an increase in vacancies in the crystal due to premelting is predicted. Because the crystalline CH_3CN unit cell consists of four differently oriented molecules, vacancy diffusion accompanying molecular reorientation is expected in the α phase. Slow vacancy diffusion was investigated by 2D exchange ^2H NMR spectra and by the stimulated-echo method.

2. Experimental Section

CD_3CN (99.8 atom % D) obtained from Aldrich Inc. was used for the measurements of ^2H NMR spectra. The ^2H NMR spectra and T_1 values were measured using a Chemagnetics CMX-300 spectrometer at 45.825 MHz. The sample temperature was controlled with a nitrogen-gas-flow temperature controller (JEOL VT1A). The temperature calibration was performed using copper−constantan thermocouples placed at the sample before NMR measurements. The temperature variation of a sample was less than 0.2 K during the measurements. The sample was sealed in a glass tube of 6-mm diameter and about 20-mm length. The 1D NMR spectra were observed using a quadrupole echo sequence $(90°)_x-\tau-(90°)_y-\tau-t_{acq}$, where τ and t_{acq} are the echo interval and acquisition time, respectively. The 90° pulse width and τ were 2.5 and 20 μs, respectively. For the measurements of a ^2H NMR stimulated echo, the pulse sequence $(90°)_x-\tau-(90°)_x-t-(90°)_x-\tau-t_{acq}$ was used.[24−26] For the measurements of 2D exchange ^2H NMR spectra, the five-pulse sequence[22] $(90°)_x-\tau-(90°)_y-\tau-t_1-(54.7°)_\varphi-t_{mix}-(54.7°)_\varphi-\tau-(90°)_y-\tau-t_2$ (acquisition) was used. The 2D spectra were recorded using 128 scans. ^2H NMR T_1 values were measured by the inversion-recovery method. Magnetization recovery was observed by using the integrated intensity of the spectrum. The

* Corresponding author. Tel.: +81 76 264 5686. Fax: +81 76 264 5742. E-mail: mizuno@wriron1.s.kanazawa-u.ac.jp.

10.1021/jp806445v CCC: $40.75
Published on Web 12/04/2008

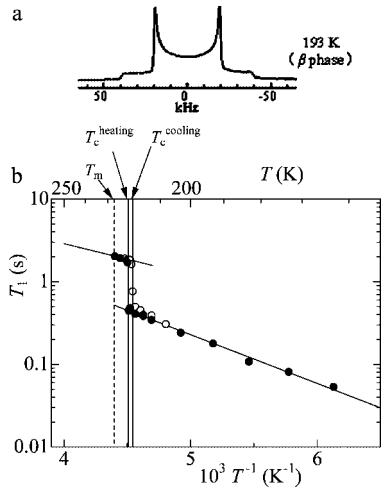

Figure 1. (a) ^{2}H NMR spectrum of the β phase and (b) temperature dependence of the ^{2}H NMR T_1 parameter for CD_3CN. Open and solid circles show the results of the heating and cooling processes, respectively.

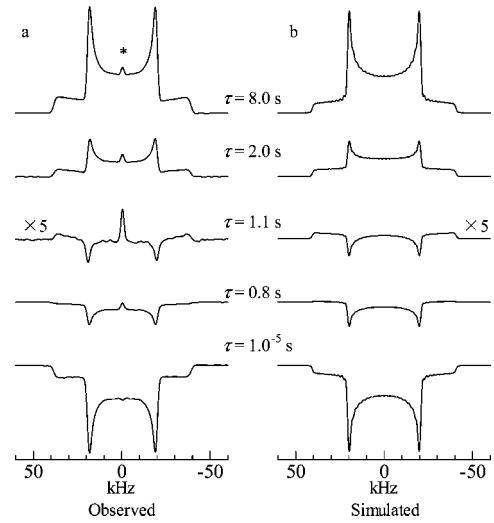

Figure 2. (a) Observed and (b) simulated partially relaxed ^{2}H NMR spectra for the measurements of T_1 using the inversion-recovery method. The spectrum was observed at 225 K (α phase). For recovery time $\tau = 1.1$ s, the spectra were scaled by a factor of 5 to reveal the line shape in the vicinity of the null. The spectral simulation was performed by assuming the three-site jump of the CD_3 group. The jumping rate of the CD_3 group and the angle between the rotation axis and the C—D bond were set to $k = 1.8 \times 10^{11}$ s^{-1} and 70°, respectively. The asterisk shows the free component due to premelting.

phase transition temperatures were determined using a differential scanning calorimeter (Rigaku Thermo Plus EVO DSC8230).

The simulations of partially relaxed ^{2}H NMR spectra for the inversion-recovery method, 2D exchange spectra, and stimulated echo were performed with homemade Fortran programs using double precision.[19]

3. Results and Discussion

Differential Scanning Calorimetry (DSC). DSC measurements were performed between 140 and 273 K. For CH_3CN, the endothermic anomaly attributed to the $\beta-\alpha$ phase transition was detected at 216.5 K and that of melting at 226.5 K during the heating process. Two exothermic anomalies were detected at 210.6 and 205.3 K during the cooling process. For CD_3CN, two endothermic anomalies attributed to the $\beta-\alpha$ phase transition and melting were detected at 222.0 and 227.0 K, respectively, during the heating process. One exothermic anomaly was detected at 209.0 K during the cooling process.

^{2}H NMR Spectroscopy. When the CD_3CN sample was cooled from room temperature, the ^{2}H NMR spectrum changed from the sharp spectrum of the liquid sample to the Pake pattern of the fine powder sample at 209 K. Figure 1a shows the broadline ^{2}H NMR spectrum observed at 193 K. The quadrupole coupling constant and the asymmetry parameter were obtained from the spectrum as $e^2qQ/h = 52.0$ kHz and $\eta = 0.0$, respectively. From these values, the electric field gradients (EFGs) at the deuterons were found to be averaged by the fast rotation of the CD_3 group about the C_3 axis. For axially symmetric C—D bond ($\eta = 0.0$), the quadrupole coupling constant averaged by the fast rotation of the CD_3 group, $(e^2qQ/h)_{av}$, can be written in terms of the static quadrupole coupling constant, $(e^2qQ/h)_{static}$, as[7]

$$\left(\frac{e^2qQ}{h}\right)_{av} = \frac{1}{2}\left(\frac{e^2qQ}{h}\right)_{static} |3\cos^2\Theta - 1| \qquad (1)$$

where Θ is the angle between the rotation axis and the C—D bond. By assuming the static values of the quadrupole coupling constant and the asymmetry parameter for the C—D bond to be $(e^2qQ/h)_{static} = 167.0$ kHz and $\eta_{static} = 0.0$, which are typical values for the ^{2}H nucleus of the C—D bond, the angle between the C_3 axis and the C—D bond was estimated as 70°. Figure 1b shows the temperature dependence of the ^{2}H NMR T_1 value for CD_3CN. T_1 increases with increasing temperature exponentially in both the β and α phases. From the temperature dependence of T_1, the activation energies of the β and α phases were determined to be 11 and 6 kJ mol^{-1}, respectively. Figure 2 shows the partially relaxed ^{2}H NMR spectra for the measurements of T_1 using the inversion-recovery method. Figure 2a shows the spectra observed at 225 K. Figure 2b shows the spectra simulated assuming a three-site jump of the CD_3 group. The variation of the line shape of the spectrum was well explained by the anisotropy of the ^{2}H NMR T_1 parameter for the rotation about the C_3 axis of the CH_3 group.[9] From the T_1 values in the α and β phases, the rate constants, k, for the rotation about the C_3 axis of the CH_3 group were estimated.[10,19] The three-site jump around the C_3 axis of the CH_3 group with an angle between the C_3 axis and the C—D bond of 70° was assumed. Values for the quadrupole coupling constant and asymmetry parameter of $e^2qQ/h_{static} = 167$ kHz and $\eta_{static} = 0.0$, respectively, were used for the calculation. Assuming an Arrhenius-type relationship, k can be written as $k = k_0 \exp(-E_a/RT)$, where E_a and k_0 are the activation energy and the jumping rate at infinite temperature, respectively, for a three-site jump about the C_3 axis of the CH_3 group. From the temperature dependence of k, values of $k_0 = (5 \pm 2) \times 10^{12}$ s^{-1}, $E_a = 6 \pm 1$ kJ mol^{-1} and $k_0 = (2 \pm 1) \times 10^{13}$ s^{-1}, $E_a = 11 \pm 2$ kJ mol^{-1} were obtained for the α and β phases, respectively. The activation energy of the rotation about the C_3 axis of the CH_3 group in the α phase was lower than that in the β phase. The jumping rates of the CH_3 group in the α and β phases near T_c became 1.8×10^{11} and 6.2×10^{10} s^{-1}, respectively. These results reflect the fact that the mobility of the CH_3 group in the α phase is higher than in the β phase. The mean value of the distances between the H atom and the nearest N atom for the three H atoms in the CH_3 group in the β phase is longer than that in the α phase (Figure 3).[4] Thus, the difference in the packing of the CD_3CN molecules in the two phases influences the mobility of the CD_3CN molecules in each phase.

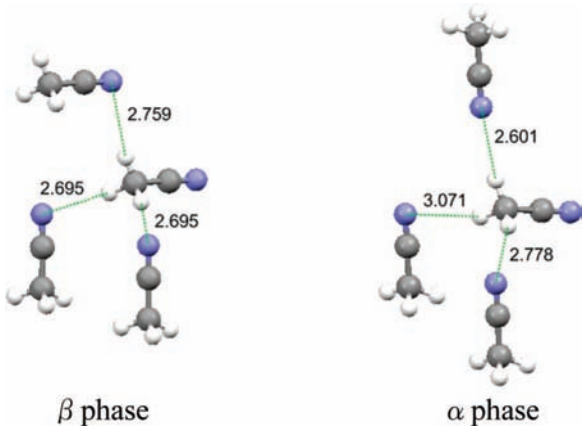

Figure 3. Distances between the H atoms and the nearest N atom in the α and β phases of CH_3CN.[4]

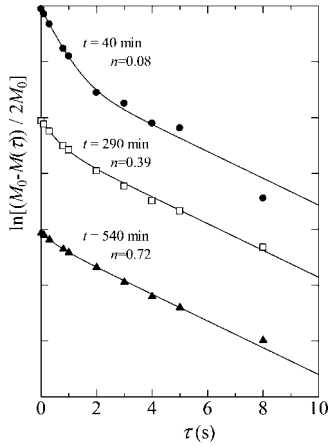

Figure 4. Time dependence of the magnetization recovery for ^{2}H NMR spectroscopy at 221 K. *t* is the time since the sample temperature had been set to 221 K. The solid lines show the fittings obtained using a double-exponential function. *n* represents the ratio of the magnetization in the α phase to the total magnetization.

Figure 4 shows the time variation of the ^{2}H NMR magnetization recovery at 221.0 K during the heating process. The magnetization recovery exhibited two components that correspond to the magnetizations in the α and β phases. The ratio of the magnetization in the α phase to the total magnetization (*n*) was estimated using the equations

$$\frac{M_0 - M(\tau)}{2M_0} = n_A \exp(-\tau/T_{1\alpha}) + n_B \exp(-\tau/T_{1\beta}) \quad (2)$$

$$n = \frac{n_A}{n_A + n_B} \quad (3)$$

where $T_{1\alpha}^{-1}$ and $T_{1\beta}^{-1}$ are the spin−lattice relaxation rates in the α and β phases, respectively. *n* increased with the passage of time. Figure 5 shows the time dependence of *n* at 221.5 and 221.0 K in the heating process. The *n* value became 1.0 within 10 min above $T_c = 222$ K. When the sample was kept at 221.5 K, however, the *n* value increased gradually and became 1.0 at 100 min. When the sample was kept at 221.0 K, the *n* value increased very slowly and became 0.72 after 540 min. During the cooling process, it took about 30 min until the T_1 value reached the value for the β phase at 220 K. A supercooling of 2 K was observed for the α−β phase transition. Thus, a slow approach to equilibrium around the β−α phase transition point was confirmed from the ^{2}H NMR magnetization recovery and T_1 value. The coexistence of the α and β phases around the

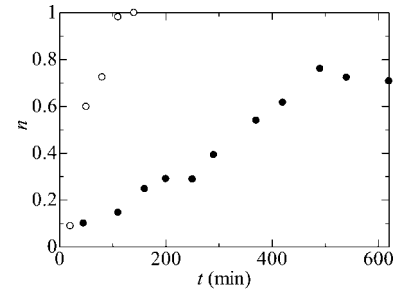

Figure 5. Time dependence of the ratio (*n*) of the magnetization in the α phase to the total magnetization around the β−α phase transition temperature in the heating process. Open and solid circles are for *n* at 221.5 and 221.0 K, respectively.

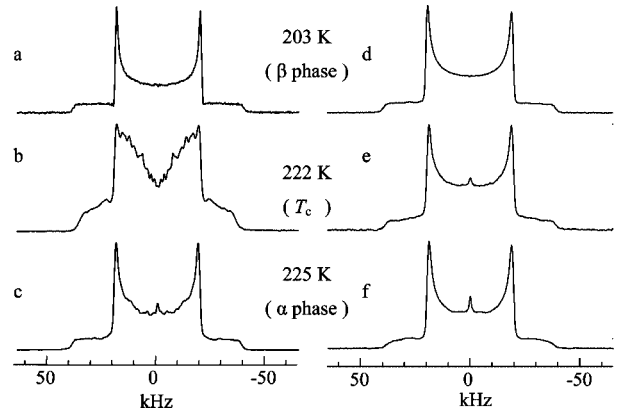

Figure 6. ^{2}H NMR spectra at 203, 222, and 225 K for samples (a−c) without and (d−f) with glass powder.

α−β phase transition point was reported from measurements of the heat capacity.[1]

Figure 6a shows the broadline ^{2}H NMR spectrum observed at 203 K, where the sample was rapidly cooled from room temperature to 203 K. Figure 6c shows the broadline ^{2}H NMR spectrum observed in the α phase (225 K), where the sample temperature was increased rapidly from 203 to 225 K. No marked change in the spectrum was observed when the sample temperature was changed rapidly from the β phase to the α phase. When the temperature was increased from the β phase to T_c, the line shape of the broadline ^{2}H NMR spectrum at T_c changed gradually for about 30 min. Figure 6b shows the broadline ^{2}H NMR spectrum at T_c (222 K), where the sample temperature was changed rapidly from 203 K to T_c and kept at T_c for 30 min. Figure 6d−f shows the broadline ^{2}H NMR spectrum of CD_3CN in the glass powder observed under the same conditions as Figure 6a−c. The weight fraction of glass powder in the sample was 0.81. The sharp component around 0 kHz appeared in the ^{2}H NMR spectrum at T_c, and its intensity increased with increasing temperature. It was found that premelting begins in the α phase. As the temperature increased rapidly from 193 K to T_c and kept at T_c, a dramatic change in the ^{2}H NMR spectrum of the sample with glass powder was not observed. The suppression of crystal growth due to the glass powder has been reported for the investigation of benzene crystal.[25] Therefore, the dramatic change in the line shape of the broadline ^{2}H NMR spectrum of the sample without glass powder at T_c is considered to be caused by the change in the molecular orientation due to crystal growth.

Figure 7 shows the ^{2}H NMR stimulated-echo decay, $F(\tau,t)$, measured at $\tau = 20$ μs in the β phase (220 K) and in the α phase (222 and 225 K). $F(\tau,t)$ of the β phase was well fitted with a single-exponential decay function. The dashed line in

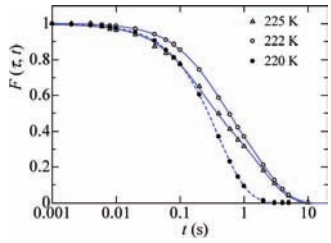

Figure 7. Stimulated-echo decay $F(\tau,t)$ of ^{2}H NMR measured at $\tau = 20\ \mu$s in the β phase (220 K, solid circles) and the α phase (222 K, open circles; 225 K, open triangles). Least-squares fitting calculations were performed using a single-exponential function for the data for the β phase (dashed line) and using eq 4 for the data for the α phase (solid lines). $F(\tau,t)$ values were normalized to $F(\tau,t = 0.001\ \text{s}) = 1.0$.

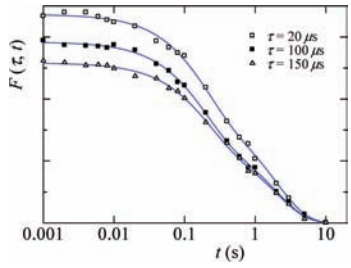

Figure 8. Stimulated-echo decay $F(\tau,t)$ of ^{2}H NMR response measured at 225 K for $\tau = 20$, 100, and 150 μs. The solid lines show the results of least-squares fitting calculations using eq 4.

Figure 7 shows the result of the least-squares fitting using $F(\tau,t) = ae^{-t/T_1}$. In the α phase, $F(\tau,t)$ deviates from the single-exponential decay and indicates a two-step decay, where the fast process is due to motion and the slow process is due to relaxation. $F(\tau,t)$ of the α phase was well explained by the equation[24−28]

$$F(\tau,t) = [A(\tau)e^{-t/\tau_c(\tau)} + B(\tau)]e^{-t/T_1} \quad (4)$$

where $\tau_c(\tau)$ is the correlation time for the molecular jump. The least-squares fitting calculation was performed using eq 4 with $A(\tau)$, $B(\tau)$, $\tau_c(\tau)$, and T_1 as parameters. $\tau_c(\tau)$ of the molecular motion in the α phase was estimated as 330 and 200 ms at 222 and 225 K, respectively. Thus, the occurrence of a slow molecular motion on the time scale of a few hundred milliseconds in the α phase was clarified from the ^{2}H NMR stimulated-echo decay.

Figure 8 shows $F(\tau,t)$ measured at 225 K for $\tau = 20$, 100, and 150 μs. The solid lines in Figure 8 show the results of the least-squares fitting using eq 4. $\tau_c(\tau)$ obtained from the fitting calculation was constant (200 ± 20 ms). Therefore, a clean large angle jump process is suggested for the slow molecular motion in the α phase.

Figure 9 shows the 2D exchange ^{2}H NMR spectra for a mixing time of $t_{mix} = 500$ ms at 222 K (α phase) and 218 K (β phase). The off-diagonal component, which consisted two ellipses, was observed in the 2D exchange ^{2}H NMR spectrum of the α phase. However, the pronounced off-diagonal component was not observed in the 2D exchange ^{2}H NMR spectrum of the β phase. These results reveal the occurrence of slow reorientational motion of CH_3CN in the α phase. The angle of reorientation, θ_{re}, is related to the shape of the off-diagonal component as[7,21]

$$|\tan \theta_{re}| = b/a \quad (5)$$

where a and b are the small and large diameters of the ellipse. The angle of reorientation of CH_3CN in the α phase was

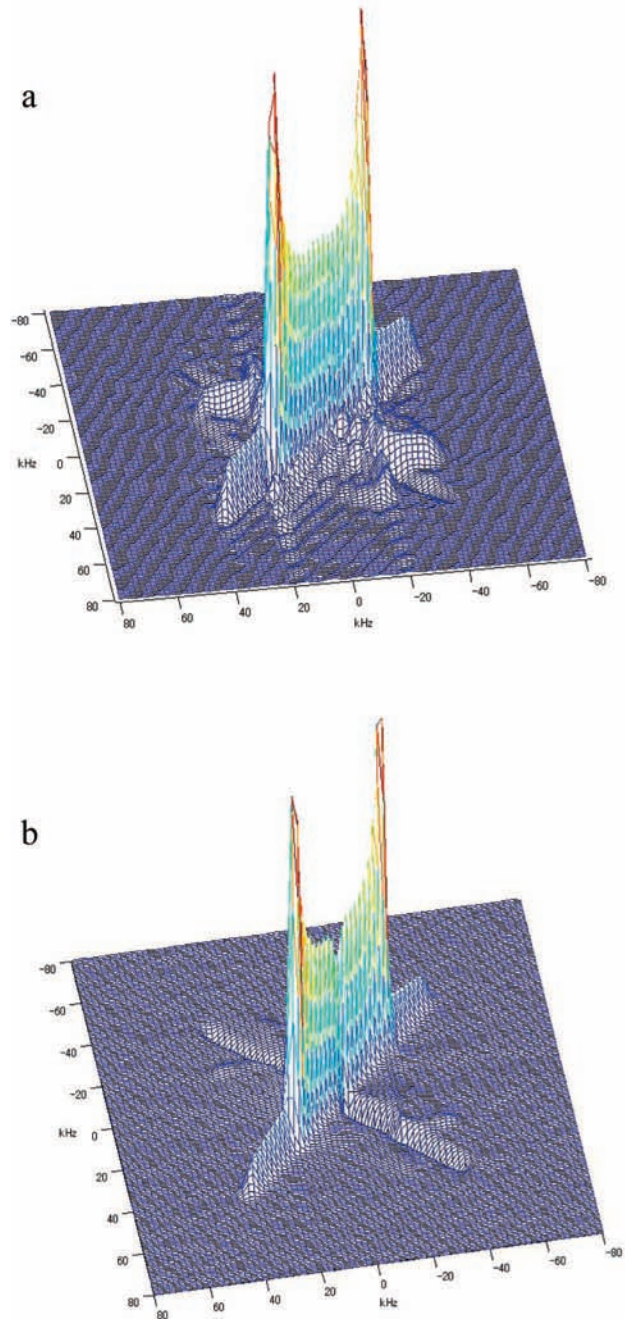

Figure 9. 2D exchange ^{2}H NMR spectra of CD_3CN for a mixing time of $t_{mix} = 500$ ms: (a) 222 K (α phase), (b) 218 K (β phase).

estimated as 76° ± 2° using eq 5. To clarify the mode of this slow motion of CH_3CN in the α phase, a spectral simulation was performed. The principal axis of the EFG tensor of the deuterons is parallel to the N—C—CH_3 molecular axis because of averaging of EFGs due to the fast rotation of the CH_3 group. As shown in Figure 10, in the α phase, four differently orientated molecules (1−4) exist in the unit cell. Sites 1 and 2 are in the same hydrogen-bond network, and sites 3 and 4 are in the nearest-neighbor hydrogen-bond network. The angles between the molecular axes of sites 1 and 2, sites 1 and 3, and sites 1 and 4 are 76.24°, 103.76°, and 180°, respectively. The jumps of CH_3CN between site 1 and site 2 ($Jump_{1-2}$) and between site 1 and site 3 ($Jump_{1-3}$) cause the reorientation of the principal axis of the EFG tensor of the deuterons, whereas no change in the EFG tensor of the deuterons is caused by the jump between sites 1 and 4 ($Jump_{1-4}$). $Jump_{1-2}$ and $Jump_{1-3}$ could not be

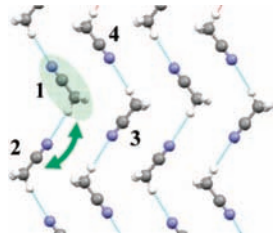

Figure 10. Model of two-site jump of CD_3CN in the α phase. Four different orientations of CD_3CN exist in the unit cell (numbered 1−4). When a vacancy is generated at site 1, the jump of CH_3CN from site 2 to the vacancy, $Jump_{1-2}$, is most probable.

distinguished by ^{2}H NMR spectrum. The angle of reorientation of CH_3CN, $\theta_{re} = 76°$, estimated by the analysis of the off-diagonal component of the 2D exchange spectrum reveals the possibility of $Jump_{1-2}$ and $Jump_{1-3}$ in the α phase. The jump of CH_3CN in the α phase is considered to occur in the presence of vacancies. Actually, the free CH_3CN component appeared in the 1D ^{2}H NMR spectra, and the creation of a vacancy is expected in the α phase. Hence, the jump of CH_3CN from the nearest-neighbor site to a vacancy in the same hydrogen-bond network, $Jump_{1-2}$, is most probable for the dynamics of CH_3CN in the α phase. Spectral simulation was performed by assuming the reorientation of the EFG tensor due to $Jump_{1-2}$.

The ^{2}H NMR frequencies at sites 1 and 2 of CH_3CN (ω_{q1}, ω_{q2}) were calculated using the equations[7−9,19,27]

$$\omega_{qi} = \sqrt{\frac{3}{2}}\sum_{n,m}^{2} D_{0n}^{(2)*}(\psi,\theta,\varphi)\, D_{n,m}^{(2)*}(\alpha_i,\beta_i,\gamma_i) T_m^{(2)} \qquad (6)$$

$$T_0^{(2)} = \sqrt{\frac{3}{8}}\frac{e^2qQ}{\hbar} \qquad T_{\pm 2}^{(2)} = \frac{\eta}{4}\frac{e^2qQ}{\hbar} \qquad (7)$$

where D is the second-order Wigner rotation matrix. (α_i, β_i, γ_i) (i = 1, 2) and (ψ, θ, φ) are the Euler angles for the transformations from the molecular axes to the principal axes of the electric field gradient tensor and from the laboratory axes to the molecular axes, respectively. The time evolution of macroscopic magnetization for the measurements of the ^{2}H NMR 2D exchange spectrum, $G(t_1,t_2,\tau,t_{mix},\theta,\varphi)$, is represented by[7,19]

$$G(t_1,t_2,\tau,t_{mix},\theta,\varphi) =$$
$$\mathbf{W}\cdot\{\hat{\mathbf{B}}_{90}{}^2 \exp(\hat{\mathbf{A}}t_2)\exp[\hat{\mathbf{A}}(\tau+t_{90})]\exp[\hat{\mathbf{A}}^*(\tau+t_{54.7})]\}\cdot$$
$$\{\hat{\mathbf{B}}_{54.7}{}^2 \exp(\hat{\mathbf{K}}t_{mix})\hat{\mathbf{B}}_{90}{}^3 \exp(\hat{\mathbf{A}}t_1)\exp[\hat{\mathbf{A}}(\tau+t_{90})]\times$$
$$\exp[\hat{\mathbf{A}}^*(\tau+t_{90})]\}\cdot\mathbf{1} \qquad (8)$$

$$\hat{\mathbf{K}} = \begin{bmatrix} -k & k \\ k & -k \end{bmatrix} \qquad \hat{\mathbf{A}} = \begin{bmatrix} -k+i\omega_{q1} & k \\ k & -k+i\omega_{q2} \end{bmatrix} \qquad (9)$$

where k is the jumping rate of CH_3CN. $\hat{B}_p$ is the effect of the pulse width of a p-degree pulse on the spectrum. **W** is the vector of site populations. The 2D exchange ^{2}H NMR signal of a powder sample was calculated as

$$G(t_1,t_2,\tau,t_{mix}) = \int_0^{2\pi}\int_0^{\pi} G(t_1,t_2,\tau,t_{mix},\theta,\varphi)\sin\theta\, d\theta\, d\varphi \qquad (10)$$

The 2D exchange ^{2}H NMR spectrum was obtained by a 2D Fourier transformation of $G(t_1,t_2,\tau,t_{mix})$. The Euler angles (α_1, β_1, γ_1) = (0°, 0°, 0°) and (α_2, β_2, γ_2) = (0°, 76.24°, 0°) were estimated from the results of X-ray diffraction.[4] The jumping rate for the two-site jump of CD_3CN was estimated as k = 1.5 s^{-1} from τ_c obtained by the ^{2}H NMR stimulated-echo decay at 222 K using the equation $k = (2\tau_c)^{-1}$. [10]

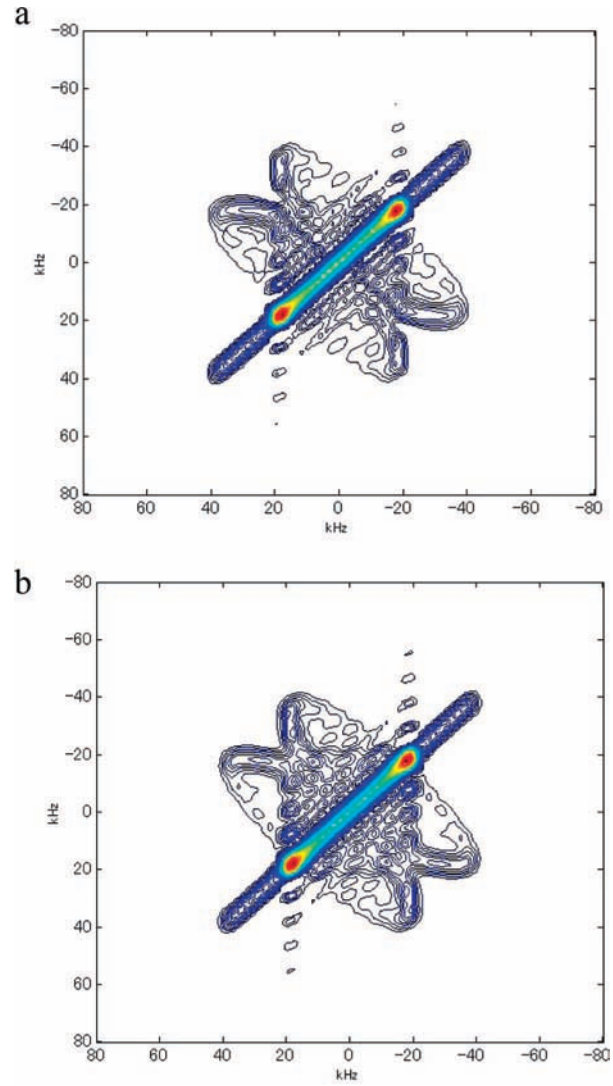

Figure 11. Contour plots of 2D exchange ^{2}H NMR spectra of CD_3CN. (a) Spectrum observed for t_{mix} = 500 ms at 222 K (same as Figure 8a) and (b) spectrum simulated by assuming a jump of CD_3CN between the nearest-neighbor sites in the hydrogen-bond network accompanying the reorientation of the molecule in the α phase. k = 1.5 s^{-1} was used for the jumping rate of CD_3CN in the spectral simulation.

Figure 11 shows contour plots of the 2D exchange ^{2}H NMR spectrum of Figure 9 and the simulated 2D exchange ^{2}H NMR spectrum. The observed spectrum was well reproduced by the spectral simulation.

The normalized final state correlation[24−26]

$$F_\infty(\tau) = \frac{F(\tau,t\to\infty)}{F(\tau,t\to 0)} \qquad (11)$$

was investigated to clarify the geometry of the molecular motion in the α phase. Figure 12 shows $F_\infty(\tau)$ observed at 225 K. The mixing times of t = 20 μs and t = 1.5 s were used for the measurements of $F(\tau,t\to 0)$ and $F(\tau,t\to\infty)$, respectively. A five-pulse sequence[22] was used, and the maximum points of the stimulated-echo signals were detected for the measurements of $F(\tau,t$ = 20 μs) and $F(\tau,t$ = 1.5 s). $F_\infty(\tau)$ was normalized to $F_\infty(0)$ = 1 in order to suppress the contribution of the spin−lattice relaxation. The large-τ limit of $F_\infty(\tau)$ became about one-half of the initial value. The ratio of the decay for $F_\infty(\tau)$ ($1/N$) corresponds to the number of sites (N) for the jump of a

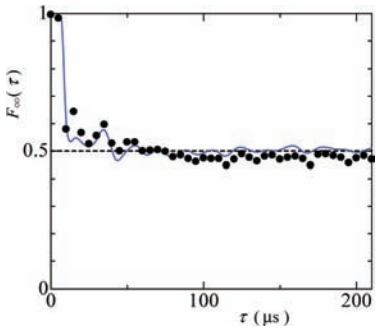

Figure 12. Normalized final state correlation, $F_\infty(\tau)$, as a function of the evolution time τ at 225 K. $F_\infty(\tau)$ was obtained as $F(\tau,t = 1.5\text{s})/F(\tau,t = 20\ \mu\text{s})$. The solid line shows the calculated value of $F_\infty(\tau)$ assuming a two-site jump of CD_3CN with the reorientation angle of θ_{re}=76.24°.

molecule.[24−26] Therefore, a two-site jump in the α phase was revealed by $F_\infty(\tau)$. Assuming a jump of CH_3CN with the reorientation angle of θ_{re}=76.24°, the ^{2}H NMR stimulated echo of a powder sample was calculated using

$$F(\tau,t) = \int_0^{2\pi}\int_0^{\pi} F(\tau,t,\theta,\varphi)\sin\theta\,\mathrm{d}\theta\,\mathrm{d}\varphi \qquad (12)$$

$$F(\tau,t,\theta,\varphi) = \mathbf{W}\cdot\exp(\hat{\mathbf{A}}\tau)\cdot[\exp(\hat{\mathbf{K}}t)\exp(\hat{\mathbf{A}}\tau)]\cdot\mathbf{1} \qquad (13)$$

For the calculation of $F(\tau,t)$, the jumping rate for the two-site jump of CD_3CN was estimated as $k = 2.5\ \text{s}^{-1}$ from τ_c obtained from the ^{2}H NMR stimulated-echo decay at 225 K using the relation $k = (2\tau_c)^{-1}$.[10] The calculated normalized final state correlation $F_\infty(\tau)$ is indicated by the solid line in Figure 12.

The present results support the existence of a jump of CH_3CN between two neighboring sites in the hydrogen-bond network. The intensity of the sharp component of the ^{2}H NMR spectrum due to the free CH_3CN increased, and the correlation time of the jump of CH_3CN obtained by the stimulated-echo decay of ^{2}H NMR decreased with increasing temperature. These results suggest that the frequency of the jump of CH_3CN in the hydrogen-bond network is enhanced by an increase in the amount of vacancies due to premelting. The jump of CH_3CN in the hydrogen-bond network observed in the ^{2}H NMR 2D exchange spectrum and the stimulated-echo decay is predicted to occur along with vacancy diffusion. From the correlation time of the jump of CH_3CN, the diffusion constant D for vacancy diffusion in the one-dimensional hydrogen-bond network can be estimated using the equation $D = \langle r^2\rangle/2\tau_c$, where $\langle r^2\rangle$ is the mean square of the distance of the molecular jump. $\langle r^2\rangle$ was estimated as 3.0×10^{-19} m^2 from the results of X-ray diffraction,[4] and τ_c was obtained from the ^{2}H NMR stimulated-echo decay in the present work. D was thus obtained as 4.5×10^{-19} and 7.5×10^{-19} m^2/s at 222 and 225 K, respectively.

4. Conclusions

The change in the mobility of the CD_3 group due to the $\alpha-\beta$ phase transition was observed using the ^{2}H NMR T_1 parameter. The difference in the mobility of the CD_3 group in the α and β phases reflects a difference in the packing of the molecules in the two phases. A jump of CH_3CN between two neighboring sites in the hydrogen network on the time scale of a few hundred milliseconds was observed in the α phase from the ^{2}H NMR 2D exchange spectrum and stimulated-echo decay. The jump of CH_3CN is closely related to vacancies in the α phase. The results of the present work strongly suggest the occurrence of vacancy diffusion in the one-dimensional hydrogen-bond network.

Acknowledgment. This work was supported by a Grant-in-Aid for Science Research in Priority Area "Chemistry of Coordination Space" (No. 434) and a Grant-in-Aid for Scientific Research (No. 19510103) from the Ministry of Education, Culture, Sports, Science and Technology, Government of Japan.

References and Notes

(1) Putnam, W. E.; McEachern, D. M.; Kilpatrick, J. E. *J. Chem. Phys.* **1965**, *42*, 749.
(2) Barrow, M. J. *Acta Crystallogr.* **1981**, *B37*, 2239.
(3) Antson, O. K.; Tilli, K. J.; Andersen, N. H. *Acta Crystallogr.* **1987**, *B43*, 296.
(4) Enjalbert, R.; Galy, J. *Acta Crystallogr.* **2002**, *B58*, 1011.
(5) Negita, H.; Casabella, P. A.; Bray, P. J. *J. Chem. Phys.* **1960**, *32*, 314.
(6) Kaplan, A.; Gattoni, A. *J. Mol. Struct.* **1980**, *58*, 283.
(7) Schmiddt-Rohr, K.; Spiess, H. W. *Multidimensional Solid-State NMR and Polymers*; Academic Press: London, 1994.
(8) Dong, R. Y. *Nuclear Magnetic Resonance of Liquid Crystals*; Springer: New York, 1997.
(9) Vold, R. R. In *Nuclear Magnetic Resonance Probes of Molecular Dynamics*; Tycko, R., Ed.; Kluwer Academic Publishers: Norwell, MA, 1994; pp 27−112.
(10) Vold, R. R.; Vold, R. L. In *Advances in Magnetic and Optical Resonance*; Warren, W. S., Ed.; Academic Press: San Diego, 1991; Vol. 16, pp 85−171.
(11) Greenfield, M. S.; Ronemus, A. D.; Vold, R. L.; Vold, R. R.; Ellis, P. D.; Raidy, T. E. *J. Magn. Reson.* **1987**, *72*, 89.
(12) Hiyama, Y.; Silverton, J. V.; Torchia, D. A.; Gerig, J. T.; Hammond, S. J. *J. Am. Chem. Soc.* **1986**, *108*, 2715.
(13) Long, J. R.; Ebelhauser, R.; Griffin, R. G. *J. Phys. Chem. A* **1997**, *101*, 988.
(14) Kimura, J.; Mizuno, M.; Suhara, M.; Endo, K. *Z. Naturforsch.* **1998**, *53a*, 453.
(15) Mizuno, M.; Hamada, Y.; Kitahara, T.; Suhara, M. *J. Phys. Chem. A* **1999**, *103*, 4981.
(16) Mizuno, M.; Iijima, T.; Suhara, M. *J. Phys.: Condens. Matter* **2000**, *12*, 7261.
(17) Iijima, T.; Mizuno, M. *Chem. Phys. Lett.* **2003**, *380*, 736.
(18) Mizuno, M.; Suzuki, Y.; Endo, K.; Murakami, M.; Tansho, M.; Shimizu, T. *J. Phys. Chem. A* **2007**, *111*, 12954.
(19) Araya, T.; Niwa, A.; Mizuno, M.; Endo, K. *Chem. Phys.* **2008**, *344*, 291.
(20) Schmidt, C.; Wefing, S.; Blümich, B.; Spiess, H. W. *Chem. Phys. Lett.* **1986**, *130*, 84.
(21) Schmidt, C.; Blümich, B.; Spiess, H. W. *J. Magn. Reson.* **1988**, *79*, 269.
(22) Schaefer, D.; Leisen, J.; Spiess, H. W. *J. Magn. Reson.* **1995**, *115A*, 60.
(23) Kuebler, S. C.; Schaefer, D. J.; Boeffel, C.; Pawelzik, U.; Spiess, H. W. *Macromolecules* **1997**, *30*, 6597.
(24) Isfort, O.; Boddenberg, B.; Fujara, F.; Grosse, R. *Chem. Phys. Lett.* **1998**, *288*, 71.
(25) Isfort, O.; Geil, B.; Fujara, F. *J. Magn. Reson.* **1998**, *130*, 43.
(26) Geil, B.; Isfort, O.; Boddenberg, B.; Favre, D. E.; Chmelka, B. F.; Fujara, F. *J. Chem. Phys.* **2002**, *116*, 2184.
(27) Medick, P.; Vogel, M.; Rössler, E. *J. Magn. Reson.* **2002**, *159*, 126.
(28) Winterlich, M.; Böhmer, R.; Diezemann, G.; Zimmermann, H. *J. Chem. Phys.* **2005**, *123*, 094504.
(29) Yang, D. K.; Zax, D. B. *Solid State Nucl. Magn. Reson.* **2006**, *29*, 153.
(30) O'Connor, R. D.; Blum, F. D.; Ginsburg, E.; Miller, R. D. *Macromolecules* **1998**, *31*, 4852.
(31) Rose, M. E. *Elementary Theory of Angular Momentum*; Wiley: New York, 1957.

JP806445V